

Aperiodic dynamical decoupling sequences in presence of pulse errors

Zhi-Hui Wang, V. V. Dobrovitski¹

¹*Ames Laboratory, Iowa State University, Ames, IA, 50011*

(Dated: May 26, 2022)

Dynamical decoupling (DD) is a promising tool for preserving the quantum states of qubits. However, small imperfections in the control pulses can seriously affect the fidelity of decoupling, and qualitatively change the evolution of the controlled system at long times. Using both analytical and numerical tools, we theoretically investigate the effect of the pulse errors accumulation for two aperiodic DD sequences, the Uhrig's DD (UDD) protocol [G. S. Uhrig, Phys. Rev. Lett. **98**, 100504 (2007)], and the Quadratic DD (QDD) protocol [J. R. West, B. H. Fong and D. A. Lidar, Phys. Rev. Lett **104**, 130501 (2010)]. We consider the implementation of these sequences using the electron spins of phosphorus donors in silicon, where DD sequences are applied to suppress dephasing of the donor spins. The dependence of the decoupling fidelity on different initial states of the spins is the focus of our study. We investigate in detail the initial drop in the DD fidelity, and its long-term saturation. We also demonstrate that by applying the control pulses along different directions, the performance of QDD protocols can be noticeably improved, and explain the reason of such an improvement. Our results can be useful for future implementations of the aperiodic decoupling protocols, and for better understanding of the impact of errors on quantum control of spins.

PACS numbers: 03.67.Pp, 03.65.Yz, 76.30.-v, 75.10.Jm

I. INTRODUCTION

Mitigating the effect of decoherence is an important problem in the emerging area of quantum information processing (QIP)¹ and other quantum-based technologies²⁻⁹. Dynamical decoupling (DD) is a promising tool for this task^{10,11}. Originating from the ideas that underlie the spin echo effect in nuclear magnetic resonance (NMR)^{12,13}, DD employs a specially designed sequence of control pulses applied to the qubits (or the central spins) in order to negate the coupling of the central spins to their environment. A variety of DD protocols have been developed, analyzed, and employed for a few decades in the area of high-resolution NMR^{14,15}. It has been suggested later that the decoupling property of these protocols can be used for more general purpose of suppressing decoherence and achieving high-fidelity quantum operations, thus giving rise to extensive theoretical^{11,16-27} and experimental²⁸⁻⁴⁰ investigation of various novel aspects of DD in the QIP context. Since DD requires no feedback and no ancilla resources, and is applicable to a wide range of systems, it presents a promising tool for lowering the number of quantum errors beyond the error correction threshold¹.

Performance analysis of the decoupling protocols is often based on the Magnus expansion (ME)¹⁴, which is an asymptotic cumulant expansion of the evolution operator of the system, with the characteristic inter-pulse delay (or duration of a single DD cycle, for periodic sequences) playing the role of the small expansion parameter. By designing the protocols which nullify more and more expansion terms, one expects that in favorable experimental situations the decoupling fidelity increases. An example of the first-order decoupling protocol is a very basic periodic dynamical decoupling (PDD) sequence^{11,41}, which consists of repeating the basic cycle $d - \pi - d - \pi$,

where d denotes the free evolution of the system, and π denotes a 180° spin rotation around e.g. x -axis (all analysis here and below is performed in the rotating frame, i.e. in the coordinate frame rotating around the z -axis with the Larmor precession frequency¹³). This sequence works for the Ising-type coupling, for instance, when a central spin is coupled to the decohering bath via the term $S^z B$, where S^z is the z -component of the central spin and B is the bath operator. Such terms lead to pure dephasing of the central spins in the x - y plane, i.e. only transverse components of the central spins are affected by the bath. In order to eliminate more general type of coupling, involving decoherence of all components of the central spin, a two-axis control is needed, when the 180° rotation axes alternate between x and y directions¹¹, so the basic period of the PDD sequence has a form $d - \pi_X - d - \pi_Y - d - \pi_X - d - \pi_Y$, with π_X and π_Y denoting the π rotations around x and y , respectively. To increase the decoupling order, eliminating the second-order ME terms as well, we need to use more advanced sequences than PDD. One possibility is to use symmetrized sequences (SDD)^{11,14,41} having a twice longer cycle, consisting of the PDD cycle followed by its mirror image. Another approach to achieve higher-order decoupling is to use concatenated DD (CDD) protocol, which removes the system-bath coupling terms in the ME up to the n -th order by nesting the PDD sequence recursively to itself n times.^{16,18,23,42} The number of pulses in CDD increases exponentially with the concatenation level, approximately as 4^n . Within CDD approach, the total decoupling time can be increased either by increasing the concatenation order, or by periodically repeating the fixed-level CDD protocol.

Another way to improve the decoupling fidelity is to optimize positions of the pulses, thus creating a family of aperiodic sequences where the inter-pulse de-

lays are not necessarily commensurate. In Ref. 19 G. S. Uhrig proposed a sequence (later abbreviated as UDD), where optimization of the pulse positions provides n -th order decoupling using n pulses^{43,44}. UDD has been implemented and tested experimentally in different systems^{31–33,36–38}. Theoretical studies have shown that UDD is optimal when the noise spectrum of the bath has a sharp high-frequency cutoff^{32,33,44}, while for the spectra with soft cutoffs the protocols with periodic structure, such as the Carr-Purcell-Meiboom-Gill¹³ (CPMG) sequence, perform better^{20,27,37,45}. While UDD employs a single-axis control, and therefore suppresses only pure dephasing, several UDD-based aperiodic protocols were developed to suppress general decoherence by incorporating double-axis controls, including the concatenated version of UDD (CUDD)⁴⁶, and quadratic DD (QDD) where two UDD sequences based on spin rotations about perpendicular axes are nested into each other²⁵. In CUDD, the number of pulses also grows exponentially but slower than CDD, and in QDD the pulse number required to suppress n -order decoherence is of order of $O(n^2)$.

While DD protocols are usually designed based on the assumption of ideal pulses, in reality the accumulation of small imperfections of the pulses can severely affect the decoupling fidelity and even qualitatively change the evolution of the central spins. The influence of the pulse errors on the DD protocols has been studied from early days of NMR^{15,47} within the ME (or ME-like) settings, by considering the pulse errors as extra terms in the Hamiltonian. However, such an approach is not always satisfactory. First, the convergence conditions of ME are not always satisfied in the experiments, although the DD may still efficiently suppresses decoherence. Second, due to its asymptotic nature, the ME can miss the possibility of disastrous pulse error accumulation at long times, when the number of pulses becomes very large. Very detailed studies of the errors introduced by the finite pulse width have been performed for CDD⁴² and UDD^{32,48}. The experimental study of the systematic errors in the rotation axis and angle has been done for a number of periodic protocols and for UDD^{36,49}, and both error types (finite-width and systematic) have been discussed for dynamically corrected gates⁵⁰. The theoretical-experimental investigation of the long-term accumulation of the systematic pulse errors has been done for several periodic-based protocols, PDD, SDD, and CDD^{40,51}.

In this work, we present a theoretical analysis of the aperiodic protocols, UDD and QDD, focusing on the long-term accumulation of the systematic pulse errors. These errors can be much more devastating than the imperfections associated with the finite width of the pulses. We use numerical modeling to analyze the situation when the aperiodic protocols with imperfect pulses are used for decoupling of the electron spins of the phosphorus donors in silicon. This system may present a promising platform for scalable solid-state quantum information processing, and is a good testbed for studying a number of fundamental issues in quantum dynamics and quantum con-

trol of solid-state spins^{52–55}. The Si:P system is well characterized^{56–59}, DD of the electron spins of P donors is efficiently implemented via pulsed ESR technique, and the realistic pulse error parameters have been estimated earlier^{40,51}. Comparing the results of our study below with the previous works on periodic protocols in the same system, we find that the aperiodic sequences provide reasonable decoupling fidelity, but they are more demanding to the pulse error magnitude than e.g. CDD. We also demonstrate that, by choosing a right set of two-axis controls, the effect of the pulse errors can be significantly reduced, and explain the reason behind this improvement. It is interesting that the right choice for QDD protocol, employing rotations around the z and y axes, is a bad choice for CDD and PDD, where the rotations around x and y should be used^{40,51}. It demonstrates again that the analysis of the pulse error accumulation is, in general, protocol-specific.

The rest of the paper is organized as follows. In Sec. II, we describe the Si:P system and present a model for the pulse errors. In Sec. III, we present the analytical and numerical results for UDD and QDD. Conclusions are given in Sec. IV.

II. DESCRIPTION OF THE SYSTEM

A. The Phosphorus Doped Silicon System

The electron spins of P donors in silicon have long relaxation and coherence times^{56–58}, and have been used earlier to explore fundamental aspects of quantum spin dynamics and DD^{29,40,51,53,58,60–62}. In this study, we consider the same experimental situation as described in Ref. 40. The sample is an isotopically purified bulk silicon with ²⁹Si concentration ~ 800 ppm, and very low doping density of phosphorus, so that the coupling between different P donor spins can be neglected at the relevant timescales. A large static (quantizing) magnetic field is applied along the z -axis to the system, and the temperature is sufficiently low (8 K in the experiments reported in Ref. 40). The relaxation time T_1 of the P electron spin is very long, so the longitudinal relaxation is neglected here. Similarly, the coherence time T_2 , defined as the spin echo decay time, is long (several milliseconds, limited by instantaneous diffusion) and will also be neglected below^{40,53,58}.

Thus, we consider only pure dephasing of the P electron spins. One important dephasing channel is the Ising-type hyperfine coupling to the ²⁹Si nuclear spins^{56–58,60,61}. Due to rather large localization radius of the P donor electron in silicon, the P electron spin couples to a large number (bath) of ²⁹Si nuclear spins. For an isotopically purified sample considered here, the interactions between different ²⁹Si nuclear spins are small and can be neglected, so we are dealing with the static nuclear spin bath. Moreover, since the P donors are well separated, the ²⁹Si nuclei which are appreciably coupled

to one P electron spin interact very weakly with other donor centers, so each donor can be considered as a separate central spin with its own static spin bath. Another important contribution to dephasing is the inhomogeneous broadening due to quasistatic fluctuations of the quantizing magnetic field. Therefore, in the frame rotating with the frequency at the center of the ESR line of the P electrons, the Hamiltonian for a P electron spin coupled to the bath is

$$\mathcal{H} = BS^z \quad (1)$$

where S^z is the z -component of the electron spin operator, and B is the total random static offset field created by the bath of ^{29}Si nuclei and the fluctuations of the external field^{13,63}. Experiments show that the ESR line-shape is Gaussian with the width of 50 mG, so that the distribution function of B is

$$P(B) = \frac{1}{\sqrt{2\pi b^2}} \exp\left[-\frac{B^2}{2b^2}\right] \quad (2)$$

with $b = 50$ mG. Note however, that our results are not very sensitive to the specific shape of the distribution. The hyperfine coupling of the P electron to the donor's own ^{31}P nuclear spin ($I = 1/2$) is large^{57,59}, of order of 100 MHz, so that the two hyperfine lines are well separated, and we assume that only one line is excited. Then the on-site hyperfine coupling to ^{31}P nucleus just shifts the ESR frequency, and we neglect this interaction.

As is standard in NMR and ESR, the experimental temperature is much larger than the Zeeman energy of the electron spins in the quantizing field. Thus, we describe the state of a P spin within the high-temperature approximation, as is customarily done in NMR/ESR theory¹³, using the density matrix $\rho \propto \mathbf{1} + \alpha S^z$, where α is small. Since the T_1 time is extremely large, and the identity matrix is not affected by the unitary evolution, we can neglect it, and consider the electron spin as being in a pure state with $S^z = 1/2$ (so-called pseudo-pure state). Other initial (pseudo)pure states, e.g. along the x and y axes, can be prepared by the $\pi/2$ pulses applied along the y and $-x$ axes, respectively. For pure initial states performance of the decoupling can be conveniently quantified by the input-output fidelity, i.e. by the overlap between the initial and the final (reduced) density matrices of the system. By virtue of the relation $\rho(t) = \frac{1}{2} + \langle S^x \rangle \sigma_x + \langle S^y \rangle \sigma_y + \langle S^z \rangle \sigma_z$, the average spin projections $\langle S^x \rangle$, $\langle S^y \rangle$, and $\langle S^z \rangle$ can be equivalently used as measures of the decoupling performance. Note that the angular brackets here denote both quantum-mechanical averaging (including trace over the bath states) and the averaging over the ensemble of different P electron spins. Below, we use the rescaled fidelity, which for the initial state along the axis $\alpha = x, y, z$ is defined as $F_\alpha = 2\langle S_\alpha \rangle$.

B. The analytical model of pulse errors

For the experimental situation under consideration the systematic errors in the pulse parameters (rotation angle and the direction of the rotation axis) are much larger than the errors associated with the finite pulse width. Therefore, we treat each π -pulse as an instantaneous but imperfect spin rotation. For a nominal π -pulse about the x axis (the π_X pulse) the unitary operator describing the spin evolution is

$$U_X = \exp[-i(\pi + \epsilon_x)(\mathbf{S} \cdot \vec{\mathbf{n}})] \quad (3)$$

where ϵ_x is the error in the rotation angle, and $\vec{\mathbf{n}} = (\sqrt{1 - n_y^2 - n_z^2}, n_y, n_z)$ is the unit vector along the rotation axis, where the small parameters n_y and n_z characterize the deviation of the actual rotation axis from the x axis. Similarly, the rotation operator for a nominal π_Y pulse is

$$U_Y = \exp[-i(\pi + \epsilon_y)(\mathbf{S} \cdot \vec{\mathbf{m}})], \quad (4)$$

where ϵ_y is the rotation angle error, and $\vec{\mathbf{m}} = (m_x, \sqrt{1 - m_x^2 - m_z^2}, m_z)$ is the actual rotation axis, with small parameters m_x and m_z . During the delay between neighboring pulses, the evolution operator is simply

$$U_d(\tau) = \exp[-iBS^z\tau] \quad (5)$$

where τ is the duration of the delay between the pulses (e.g., for periodic sequences studied in Ref. 40 equal to 11 μs).

To model the systematic errors, we take into account that the resonant ac field B_p , which rotates the spins during pulses, is not homogeneous over the sample. We assume for simplicity that this field varies only along one spatial axis, denoted as l , and the sample is located between $l = +d$ and $l = -d$. We also assume that the sample is placed optimally with respect to the field, with the sample center $l = 0$ located at the maximum of B_p . Then the spatial dependence of B_p has a form $B_p(l) = \bar{B}_p + \Delta B_p[1 - 3l^2/d^2]$, where \bar{B}_p is the average magnitude of the ac field over the sample and ΔB_p characterizes the ac field inhomogeneity. If the pulse width t_p is adjusted to give $\bar{B}_p t_p = \pi$, then the spins located at different parts of sample will undergo rotation by different angles. For π_X pulse, the resulting rotation angle errors ϵ_x will have distribution

$$P(\epsilon_x) = (1/2\epsilon_0)[3(1 - \epsilon_x/\epsilon_0)]^{-1/2}, \quad (6)$$

where $-2\epsilon_0 \leq \epsilon \leq \epsilon_0$, and ϵ_0 characterizes the magnitude of the rotation angle errors. In a similar way, we assume that the z -component of the rotation axis n_z has the same distribution, and its magnitude is characterized by the parameter n_0 . We also assume that the pulse errors for π_X and π_Y pulses are the same, taking $\epsilon_x = \epsilon_y$ and $m_z = n_z$. The pulse error parameters m_x and n_y have different

nature: they characterize the phase of the pulse, and can be adjusted very precisely, so we assume them to be zero, following Refs. 40,51. Thus, within this model, all pulse errors are characterized by only two parameters, $\epsilon_0 = 0.3$ and $n_0 = -0.12$. These values have been determined in Refs. 40,51, and have reasonable magnitude. In spite of utter simplicity, this model reproduces (or, at least, mimics) well most features observed in experiments.

III. NUMERICAL AND ANALYTICAL RESULTS

A. Performance of UDD

Uhrig's DD protocol, UDD, is based on a single-axis control, i.e., all spin rotations are performed about the same nominal axis, which we take as x . For UDD of level ℓ , denoted as UDD- ℓ , the π_X pulses are applied at times¹⁹

$$t_j = t \sin^2 \left(\frac{j\pi}{2\ell + 2} \right). \quad (7)$$

where t is the total evolution time, and $j = 1, 2, \dots, \ell$ for even ℓ and $j = 1, 2, \dots, \ell + 1$ for odd ℓ . The simulation results show that UDD of even levels and UDD of odd levels behave differently. Fig. 1 shows the decoupling fidelities for UDD- ℓ as functions of total evolution time for $\ell = 2, 20$, and Fig. 2 shows the results for UDD- ℓ with $\ell = 3$ and 19.

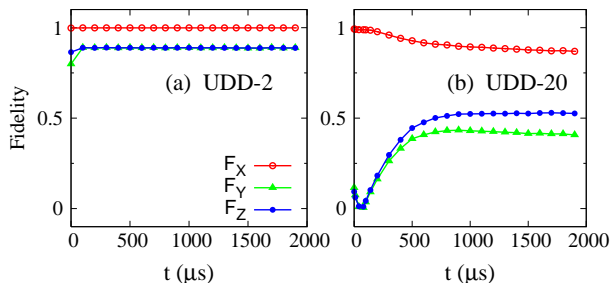


FIG. 1: (Color online). Decoupling fidelities of UDD-2 (a) and UDD-20 (b) as functions of the total evolution time for initial states S_X (red empty circles, red lines), S_Y (green triangles, green lines), and S_Z (blue solid circles, blue lines).

We consider fidelities for three different initial states of the central spins, directed along x , y , and z axes. They characterize how well the corresponding spin components are preserved. For UDD-2, which is the same as a single cycle of CPMG, the spin component S_X is preserved with fidelity close to 1, while the fidelities for the other two components are affected by the pulse errors. For long evolution time, F_Y and F_Z saturate at values ~ 0.89 . Strong dependence of the fidelity on the initial state has been noticed and analyzed before for periodic protocols, and it is not unexpected that aperiodic sequences demonstrate

this feature as well^{23,36,40,51}. For $\ell = 20$, S_X is well preserved, demonstrating only a slow decay, while F_Y and F_Z have initial values close to zero, and saturate to a value around 0.5. Such low values even for $t = 0$ are caused purely by a catastrophic accumulation of errors of 20 π_X pulses.

Let us consider the level-2 UDD as an example in order to examine the long time behavior. The evolution operator, up to second order in the pulse errors, and using $n_y = 0$, is

$$U_2^{\text{UDD}} = -[1 - \theta_x^2/2 - i\sigma_x\theta_x - i\sigma_z\theta_z] \quad (8)$$

with $\theta_x = \epsilon_x \cos \frac{Bt}{4} + 2n_z \sin \frac{Bt}{4}$ and $\theta_z = \epsilon_x n_z \cos \frac{Bt}{2} + (n_z^2 - \frac{\epsilon_x^2}{4}) \sin \frac{Bt}{2}$. Although the qualitative features of the protocol can be analyzed using only the first-order expression for U^{UDD} , quantitative analysis of the fidelity requires the second-order terms in this evolution operator. Taking into account that ϵ_x , n_z , and B are independent variables, and that $\langle \epsilon_x \rangle = \langle n_z \rangle = 0$, the expression for F_y becomes

$$\begin{aligned} F_y &= 1 - 2\theta_x^2 \\ &= 1 - 2[\langle \epsilon_x^2 \rangle \langle \cos^2 \frac{Bt}{4} \rangle + 4\langle n_z^2 \rangle \langle \sin^2 \frac{Bt}{4} \rangle]. \end{aligned} \quad (9)$$

Noticing from Eq. (6) that $\langle \epsilon_x^2 \rangle = 0.8\epsilon_0^2$, and $\langle n_z^2 \rangle = 0.8n_0^2$, we arrive at

$$\lim_{t \rightarrow \infty} F_y = 1 - 0.8(\epsilon_0^2 + 4n_0^2) = 0.88 \quad (10)$$

This is close to the value 0.89 which we see in the simulations shown in Fig. 1 for UDD-2. The analysis above relies on the fact that B is time-independent, so in experiments such saturations will be replaced by decays at different rates, depending on the bath dynamics. Therefore, although our results extend until $t = 2000 \mu\text{s}$, at these times the instantaneous diffusion and the internal bath dynamics should be taken into account. We neglect these effects here since they are beyond the scope of our present study, and require a separate focused research effort.

For UDD of higher level, similar behavior is observed. In Fig. 1, the fidelities for UDD-20 are generally smaller than for UDD-2, which reflects more serious accumulation of the pulse errors.

An interesting feature, seen in Fig. 1, is that at longer times, when dephasing becomes noticeable, the fidelities may increase, as if decoherence counteracts the pulse errors. To understand this, let us consider UDD-2 in the situation when the errors n_z are absent, and only the rotation angle error ϵ_x is nonzero. If a spin is prepared along the y axis, and is subjected to a sequence of imperfect π_X pulses, then its y -component rotates around the x -axis, and accumulates the rotation angle errors. But if the random field B moved the spin away from the y -axis towards the x -axis by the angle $\chi = Bt/4$, then the spin component along the x axis is not affected by the rotation

angle errors, and the spin is refocused with better precision. Correspondingly, the fidelity for a fixed value of B demonstrates a modulation proportional to $-\cos^2 \chi$, with maximum fidelity achieved at $\chi = \pi/2$.

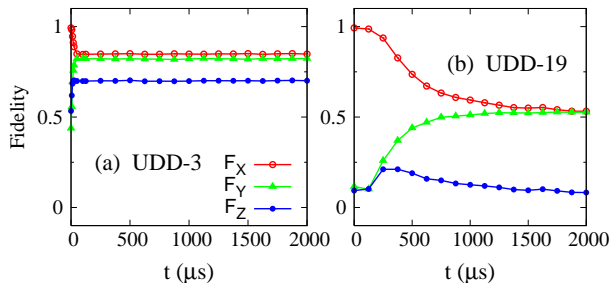


FIG. 2: (Color online). Decoupling fidelities of UDD-3 (a) and UDD-19 (b) as functions of the total evolution time for initial states S_X (red empty circles, red lines), S_Y (green triangles, green lines), and S_Z (blue solid circles, blue lines).

For UDD of odd level $\ell = 2n - 1$, the number of pulses is $2n$ since there is a π pulse at the end of the whole evolution. As shown in Fig. 2, for a given UDD- ℓ , when the total evolution time is short, S_X is better preserved than the other two spin components. At long time, F_x and F_y saturate at similar values, while F_z saturates at a lower value. The process of saturation is much slower for $\ell = 19$ than for $\ell = 3$.

To gain insight into the behavior of odd-level UDD, we consider UDD-3. The evolution operator for this sequence, up to first order in the pulse errors, is

$$U_3^{\text{UDD}} = \mathbf{1} - i\theta_n \sigma_x - i\eta_n \sigma_y \quad (11)$$

with

$$\begin{aligned} \theta_n &= \frac{\epsilon_x}{2} [1 + 2 \cos(B\tau_1) + \cos(B(\tau_2 - \tau_1))] \\ &+ n_z [2 \sin(B\tau_1) + \sin(B(\tau_2 - \tau_1))] \end{aligned} \quad (12)$$

and

$$\begin{aligned} \eta_n &= -n_z [1 - 2 \cos(B\tau_1) + \cos(B(\tau_2 - \tau_1))] \\ &- \frac{\epsilon_x}{2} [2 \sin(B\tau_1) - \sin(B(\tau_2 - \tau_1))] , \end{aligned} \quad (13)$$

where τ_1 and τ_2 refer to the durations of the first and second inter-pulse delays. In general, for quantitative calculation of the fidelities, we need also to consider the second-order terms, but it can be shown that for UDD-3 their contribution is zero. At long times, when $\langle \sin(B\tau_1) \rangle = \langle \sin(B(\tau_2 - \tau_1)) \rangle = 0$ (and similarly for cosines), the fidelity F_y acquires a form

$$\begin{aligned} F_y &= 1 - 2\langle \theta_n^2 \rangle \\ &= 1 - 2\langle 5n_z^2 + \frac{\epsilon_x^2}{4} + (\frac{\epsilon_x^2}{4} - n_z^2) \left(4 \cos^2(B\tau_1) \right. \\ &\quad \left. + \cos^2(B(\tau_2 - \tau_1)) \right) \rangle \end{aligned} \quad (14)$$

and we finally obtain

$$\lim_{t \rightarrow \infty} F_y = 1 - 5\langle n_z^2 \rangle - \frac{7\langle \epsilon_x^2 \rangle}{4} = 0.82, \quad (15)$$

which coincides with the result of the numerical simulations.

We now examine the fidelities at $t \rightarrow 0$. Since we treat pulses as instantaneous rotations, this situation should be understood as the limit where the total evolution time is much smaller than the dephasing time $T_2^* = 1/b$, but much larger than the total width $2nt_p$ of all pulses. Decay of fidelity in this case arises only from accumulation of the pulse errors. The evolution operators for UDD of both even ($\ell = 2n$) and odd ($\ell = 2n - 1$) levels have the same expression

$$\lim_{t \rightarrow 0} U_\ell^{\text{UDD}} = (-1)^n (1 - in\epsilon_x \sigma_x), \quad (16)$$

corresponding to a spin rotation about the x axis with the rotation angle proportional to n . Small differences in the rotation angles for different spins are scaled by n . For large n the spins become almost uniformly distributed in the y - z plane, hence F_y and F_z are close to zero, while F_x is close to 1, as seen in Figs. 1 and 2 for $\ell = 20$ and $\ell = 19$.

B. Performance of QDD

In order to suppress general decoherence, DD sequence has to use two-axis control. An extension of UDD, the quadratic DD (QDD) has been suggested for this purpose²⁵. QDD is composed of two nested UDD sequences, with inner and outer sequences employing the rotations about two different perpendicular axes. A QDD sequence of order ℓ , which we denote as QDD- ℓ , can suppress decoherence to ℓ -th order terms with $(\ell + 1)^2$ inter-pulse intervals.

1. QDD based on π_X and π_Y pulses

We first consider the QDD sequence with the π_X pulses in the outer hierarchical level, and π_Y pulses in the inner hierarchical level, examining the effects of error accumulation.

Like UDD, QDD of even and odd levels also behave differently. For $\ell = 2n - 1$, the sequence of QDD- ℓ is

$$\text{UDD}_\ell^{(Y)}(\tau_1) - \pi_X - \text{UDD}_\ell^{(Y)}(\tau_2) - \pi_X \cdots - \text{UDD}_\ell^{(Y)}(\tau_{\ell+1}) - \pi_X \quad (17)$$

where $\sum_{j=1}^{\ell+1} \tau_j = t$ and $\text{UDD}_\ell^{(Y)}(\tau_j)$ denotes UDD- ℓ based on π_Y pulses with evolution time τ_j . The division of the total time t into intervals τ_j follows the same rule as UDD, i.e., $\tau_j = t_j - t_{j-1}$, with t_j given by Eq. (7). The number of pulses in QDD with $\ell = 2n - 1$ is $(\ell + 1)(\ell + 2)$.

For $\ell = 2n$ the sequence QDD- ℓ is

$$\text{UDD}_\ell^{(Y)}(\tau_1)\text{-}\pi_X\text{-}\dots\text{-}\text{UDD}_\ell^{(Y)}(\tau_\ell)\text{-}\pi_X\text{-}\text{UDD}_\ell^{(Y)}(\tau_{\ell+1}) \quad (18)$$

and the number of pulses is $\ell(\ell + 2)$.

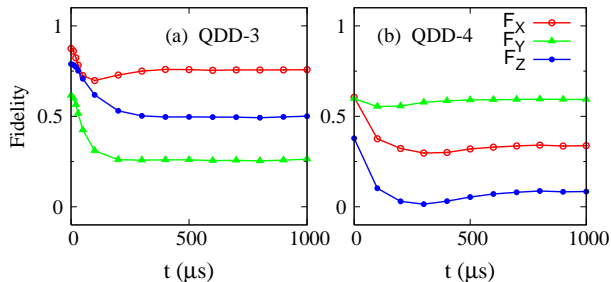


FIG. 3: (Color online). Decoupling fidelities as functions of the total evolution time for initial states S_X (red empty circles, red lines), S_Y (green triangles, green lines), and S_Z (blue solid circles, blue lines). (a) QDD-3 (20 pulses). (b) QDD-4 (24 pulses).

Considering the limit $t \rightarrow 0$, we have for even and odd levels

$$\lim_{t=0} U_{2n}^{\text{QDD}} = 1 - in(\epsilon_x \sigma_x + \epsilon_y \sigma_y) \quad (19)$$

$$\lim_{t=0} U_{2n-1}^{\text{QDD}} = (-1)^n (1 - in\epsilon_x \sigma_x) \quad (20)$$

That is, for short total evolution time, in a sequence QDD- $(2n)$, the dominant pulse error is ϵ_x , while in QDD- $(2n - 1)$ both ϵ_x and ϵ_y contribute in first order. The difference is due to an extra π_X pulse at the end of the odd-order QDD.

Simulation results for QDD-3 are shown in Fig. 3 (a). Fidelities for all three spin components exhibit long-time saturation. The saturation value for S_X is higher than for the other two components. However, F_x in QDD-3 exhibits initial decay (even for $t = 0$), instead of being preserved as expected from Eq. (20). This is because for the system under consideration, the error parameter $\epsilon_0 = 0.3$ is pretty large, and the pulse errors may appreciably contribute in higher orders. Taking QDD of $\ell = 3$ as an example, in the limit $t \rightarrow 0$, the sequence is a fourfold repetition of the unit

$$(\pi_Y\text{-}\pi_Y\text{-}\pi_Y\text{-}\pi_Y)\text{-}\pi_X. \quad (21)$$

Expanding the corresponding evolution operator up to second order in the pulse errors, and taking into account $m_x = n_y = 0$, we find that

$$U = (1 - 2\epsilon_x^2) - 2i\epsilon_x \sigma_x + 2i\epsilon_x(2\epsilon_y + n_z) \sigma_z. \quad (22)$$

Thus, the rotation axis deviates from the x axis towards the z axis, and the spin state along the x axis is not exactly parallel to the rotation axis, resulting in the initial drop of F_x .

Fig. 3 (b) shows the simulation results for QDD-4, with 24 pulses. The saturation values in a descending order

are F_y , F_x and F_z . The initial values for F_x and F_y are the same, which can be explained by Eq. (19) taking into consideration that $\epsilon_x = \epsilon_y$ in our model.

As we see, the QDD sequences are rather sensitive to the pulse errors. While the saturation at long times is seen for all spin components, the initial fidelity loss is noticeable.

2. QDD based on π_Z and π_Y pulses

In order to further understand the effect of pulse errors, we briefly consider another QDD sequence with π_Z pulses in the outer hierarchical level and π_Y pulses in the inner one. We denote such a sequence as QDD(ZY). To produce π_Z pulses in ESR experiments, the pulses π_X and π_Y are applied back-to-back⁴⁰, and our simulations reproduce this situation, taking into account the π_X and π_Y pulse errors. Fig. 4 shows the simulation results for QDD(ZY) of levels 3 and 5 (two upper panels), and 2 and 4 (two lower panels), with 20 and 42, and 8 and 24 pulses, respectively. While QDD(ZY) of even levels provide no obvious improvement compared to QDD sequences based on π_X and π_Y pulses, the QDD(ZY) protocols of odd level preserve all three spin components, with high saturation values at long times.

To understand this effect, let us inspect the structure of the QDD(ZY) sequence. As seen from Eq. (17), since UDD of odd level has a π -pulse at the end of the sequence, after nesting this π_Y pulse is followed by a π_Z pulse without delay, and these two adjacent pulses are equivalent to a (imperfect) π_X pulse. The sequence of QDD(ZY) thus has a structure

$$\begin{aligned} &(\tau_{1,1}\text{-}\pi_Y\text{-}\tau_{1,2}\text{-}\pi_Y\text{-}\tau_{1,3}\text{-}\pi_Y\text{-}\tau_{1,4})\text{-}\pi_X\text{-} \\ &(\tau_{2,1}\text{-}\pi_Y\text{-}\tau_{2,2}\text{-}\pi_Y\text{-}\tau_{2,3}\text{-}\pi_Y\text{-}\tau_{2,4})\text{-}\pi_X\text{-} \\ &(\tau_{3,1}\text{-}\pi_Y\text{-}\tau_{3,2}\text{-}\pi_Y\text{-}\tau_{3,3}\text{-}\pi_Y\text{-}\tau_{3,4})\text{-}\pi_X\text{-} \\ &(\tau_{4,1}\text{-}\pi_Y\text{-}\tau_{4,2}\text{-}\pi_Y\text{-}\tau_{4,3}\text{-}\pi_Y\text{-}\tau_{4,4})\text{-}\pi_X \end{aligned} \quad (23)$$

where $\tau_{i,j}$ denotes the j -th delay in the i -th UDD in the whole sequence. Therefore, QDD(ZY) of odd level is actually based on pulses about x and y axes, and has a structure similar to the periodic sequences based on x and y rotations, which are known to be very robust with respect to the pulse errors^{37,38,40,45,51,64}. Such a structure can not be achieved with QDD based on π_X and π_Y pulses. At even level, the x, y -based QDD lacks a final π_X pulse, see Eq. 18. At odd level, the x, y -based QDD has even number of π_Y pulses sandwiched by π_X pulses, see Eqs. 17 and 21, while for robustness we need odd number of y -pulses.

In the limit $t \rightarrow 0$, to first order in the pulse errors, the evolution operator for QDD(ZY) of level $\ell = 2n - 1$ is

$$U_{\ell=2n-1}^{\text{QDD(ZY)}} = (-1)^n [1 + 2in(m_x + n_y)\sigma_z]. \quad (24)$$

Since for our system $m_x = n_y = 0$, the DD performance is determined by accumulation of the higher-order errors.

Therefore, for QDD(ZY) of odd level, the dominant pulse errors are the in-plane components of rotation axis errors. For the system under consideration such errors are negligible, and QDD(ZY) is a good choice for decoherence suppression for all quantum states.

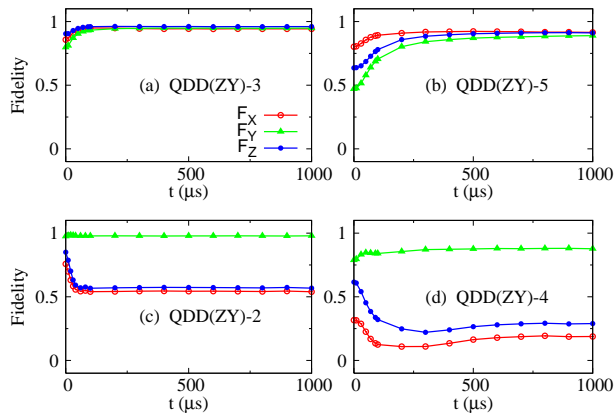


FIG. 4: (Color online). Decoupling fidelities for QDD(ZY) as functions of the total evolution time for initial states S_X (red empty circles, red lines), S_Y (green triangles, green lines), and S_Z (blue solid circles, blue lines). (a) level 3 QDD(ZY), (b) level 5 QDD(ZY), (c) level 2 QDD(ZY), (d) level 4 QDD(ZY).

IV. CONCLUSION

We have studied accumulation of the pulse errors for two aperiodic dynamical decoupling sequences, UDD and

QDD, using the phosphorus electron spins in silicon as an example of experimental implementation. We show that the decoupling fidelity strongly depends on the initial state. At long times, we observe saturation of fidelities. UDD and QDD of even and odd levels are found to perform differently.

UDD protocol is based on a single-axis control, so the decoupling fidelity is highest for the spin component along the control axis. QDD preserves the three spin states with closer fidelities. In particular, QDD of odd level based on π_Z and π_Y pulses is very robust with respect to the pulse errors, due to its special structure. Our results can be useful for experimental implementations of the aperiodic decoupling protocols, and for deeper understanding of the influence of errors on quantum control of spin systems.

Acknowledgments

We would like to thank K. Khodjasteh and L. Viola for useful discussions, and A. M. Tyryshkin and S. A. Lyon for useful discussions and stimulating suggestions. Work at the Ames Laboratory was supported by the Department of Energy – Basic Energy Sciences under Contract No. DE-AC02-07CH11358.

-
- ¹ M. A. Nielsen, I. L. Chuang, *Quantum Computations and Quantum Information* (Cambridge Univ. Press, Cambridge, 2002).
 - ² L. Childress, J. M. Taylor, A. S. Sorensen, and M. D. Lukin, Phys. Rev. Lett. **96**, 070504 (2006).
 - ³ J. A. Jones *et al.*, Science **324**, 1166 (2009).
 - ⁴ P. Cappellaro, J. Emerson, N. Boulant, C. Ramanathan, S. Lloyd, and D. G. Cory, Phys. Rev. Lett. **94**, 020502 (2005).
 - ⁵ J. M. Geremia, J. K. Stockton, and H. Mabuchi, Phys. Rev. Lett. **94**, 203002 (2005).
 - ⁶ J. M. Taylor, P. Cappellaro, L. Childress *et al.*, Nature Phys. **4**, 810 (2008).
 - ⁷ C. Degen, Appl. Phys. Lett. **92**, 243111 (2008).
 - ⁸ G. Balasubramanian, I.-Y. Chan, R. Kolesov *et al.*, Nature **455**, 648 (2008).
 - ⁹ G. de Lange, D. Ristè, V. V. Dobrovitski, R. Hanson, arXiv:1008.4395.
 - ¹⁰ L. Viola and S. Lloyd, Phys. Rev. A **58**, 2733 (1998).
 - ¹¹ L. Viola, S. Lloyd, and E. Knill, Phys. Rev. Lett. **83**, 4888 (1999).
 - ¹² E. Hahn, Phys. Rev. **80**, 580 (1950).
 - ¹³ C. P. Slichter, *Principles of Magnetic Resonance* (Springer, Berlin, New York, 1990).
 - ¹⁴ U. Haeberlen, *High Resolution NMR in solids: Selective Averaging* (Academic Press, New York, 1976).
 - ¹⁵ B. C. Gerstein and C. R. Dybowski, *Transient Techniques in NMR of Solids* (Academic Press, Orlando, 1985).
 - ¹⁶ K. Khodjasteh and D. A. Lidar, Phys. Rev. Lett. **95**, 180501 (2005).
 - ¹⁷ Ren-Bao Liu, Wang Yao, L. J. Sham, New J. Phys. **9**, 226 (2007).
 - ¹⁸ W. X. Zhang, V. V. Dobrovitski, L. F. Santos, L. Viola, and B. N. Harmon, Phys. Rev. B **75**, 201302(R) (2007).
 - ¹⁹ G. S. Uhrig, Phys. Rev. Lett. **98**, 100504 (2007).
 - ²⁰ L. Cywinski, R. M. Lutchyn, C.P. Nave, S. Das Sarma, Phys. Rev. B **77**, 174509 (2008).
 - ²¹ L. Cywinski, W. M. Witzel, and S. Das Sarma, Phys. Rev. B **79**, 245314 (2009).
 - ²² G. S. Uhrig, New J. Phys. **10**, 083024 (2008).
 - ²³ W. Zhang, N. P. Konstantinidis, V. V. Dobrovitski, B. N. Harmon, L. F. Santos, and L. Viola, Phys. Rev. B **77**, 125336 (2008).
 - ²⁴ W. Zhang, N. P. Konstantinidis, K. Al-Hassanieh, V. V. Dobrovitski, J. Phys.: Cond. Matter **19**, 083202 (2007).
 - ²⁵ J. R. West, B. H. Fong and D. A. Lidar, Phys. Rev. Lett. **104**, 130501 (2010).
 - ²⁶ K. Khodjasteh, D. A. Lidar, and L. Viola, Phys. Rev. Lett.

- 104**, 090501 (2010).
- ²⁷ S. Pasini and G. S. Uhrig, Phys. Rev. A **81**, 012309 (2010).
- ²⁸ E. Fraval, M. J. Sellars, and J. J. Longdell, Phys. Rev. Lett. **95**, 030506 (2005).
- ²⁹ J. J. L. Morton *et al.*, Nature (London) **455**, 1085 (2008).
- ³⁰ D. Press, T. D. Ladd, B. Zhang, Y. Yamamoto, Nature **456**, 218 (2008).
- ³¹ H. Uys, M. J. Biercuk, and J. J. Bollinger, Phys. Rev. Lett. **103**, 040501 (2009).
- ³² M. J. Biercuk, H. Uys, A. P. Vandevender, N. Shiga, W. M. Itano, and J. J. Bollinger, Nature (London) **458**, 996 (2009).
- ³³ J. Du, X. Rong, N. Zhao, Y. Wang, J. Yang and R. B. Liu, Nature **461**, 1265 (2009).
- ³⁴ V. V. Dobrovitski, G. de Lange, D. Riste, R. Hanson, Phys. Rev. Lett. **105**, 077601 (2010) .
- ³⁵ B. Naydenov *et al.*, arXiv:1008.1953v2 (2010).
- ³⁶ G. A. Alvarez, A. Ajoy, X. Peng, and D. Suter, Phys. Rev. A **82**, 042306 (2010).
- ³⁷ G. de Lange, Z. H. Wang, D. Risté, V. V. Dobrovitski, R. Hanson, Science **330**, 60 (2010).
- ³⁸ C. A. Ryan, J. S. Hodges and D.G. Cory, Phys. Rev. Lett. **105**, 200402 (2010).
- ³⁹ H. Bluhm *et al.*, arXiv:1005.2995v1 (2010).
- ⁴⁰ A. M. Tyryshkin, Zhi-Hui Wang, Wenxian Zhang, E. E. Haller, J. W. Ager, V. V. Dobrovitski, S. A. Lyon, arXiv:1011.1903v2.
- ⁴¹ L. F. Santos and L. Viola, Phys. Rev. A **72** 062303 (2005).
- ⁴² K. Khodjasteh and D. A. Lidar, Phys. Rev. A **75**, 062310 (2007).
- ⁴³ B. Lee, W. M. Witzel, and S. Das Sarma, Phys. Rev. Lett. **100**, 160505 (2008).
- ⁴⁴ W. Yang and R.-B. Liu, Phys. Rev. Lett. **101**, 180403 (2008).
- ⁴⁵ Ashok Ajoy, Gonzalo A. Alvarez, Dieter Suter, arXiv:1011.6243v2.
- ⁴⁶ G. S. Uhrig, Phys. Rev. Lett. **102**, 120502 (2009).
- ⁴⁷ R. W. Vaughan, D. D. Elleman, L. M. Stacey, W.-K. Rhim, J. W. Lee, Rev. Sci. Instr. **43**, 1356 (1972).
- ⁴⁸ G. S. Uhrig, S. Pasini, New J. Phys. **12**, 045001 (2010).
- ⁴⁹ M. J. Biercuk, H. Uys, A. P. VanDevender, N. Shiga, W. M. Itano, and J. J. Bollinger, Phys. Rev. A **79**, 062324 (2009).
- ⁵⁰ K. Khodjasteh, L. Viola, Phys. Rev. A **80**, 032314 (2009).
- ⁵¹ Zhi-Hui Wang, Wenxian Zhang, A. M. Tyryshkin, S. A. Lyon, J. W. Ager, E. E. Haller, and V. V. Dobrovitski, arXiv:1011.6417v1.
- ⁵² B. E. Kane, Nature **393**, 133 (1998).
- ⁵³ A. M. Tyryshkin *et al.*, J. Phys.: Cond. Matter **18**, 783 (2006).
- ⁵⁴ A. R. Stegner *et al.*, Nature Phys. **2**, 835 (2006).
- ⁵⁵ A. Morello *et al.*, arXiv:1003.2679 (2010).
- ⁵⁶ A. Honig and J. Combrisson, Phys. Rev. **102**, 917 (1956).
- ⁵⁷ G. Feher and E. A. Gere, Phys. Rev. **114**, 1245 (1959).
- ⁵⁸ A. M. Tyryshkin, S. A. Lyon, A. V. Astashkin and A. M. Raitsimring, Phys. Rev. B **68**, 193207 (2003).
- ⁵⁹ R. C. Fletcher, W. A. Yager, G. L. Pearson, F. R. Merritt, Phys. Rev. **95**, 844 (1954).
- ⁶⁰ R. de Sousa and S. Das Sarma, Phys. Rev. B **68**, 115322 (2003).
- ⁶¹ W. M. Witzel, R. de Sousa, and S. Das Sarma, Phys. Rev. B **72**, 161306(R) (2005).
- ⁶² W. M. Witzel, M. S. Carroll, A. Morello, L. Cywiński, S. Das Sarma, Phys. Rev. Lett. **105**, 187602 (2010).
- ⁶³ A. Abragam, *Principles Of Nuclear Magnetism* Clarendon, Oxford, England, 1961.
- ⁶⁴ T. Gullion, D. B. Baker, M. S. Conradi, J. Mag. Res. **89**, 479 (1990).